


 Cite this: *RSC Adv.*, 2021, 11, 10381

Received 4th February 2021

Accepted 5th March 2021

DOI: 10.1039/d1ra00943e

rsc.li/rsc-advances

High NH₃-SCR reaction rate with low dependence on O₂ partial pressure over Al-rich Cu-*BEA zeolite†

 Yusuke Ohata,^a Takeshi Ohnishi,^a Takahiko Moteki^{ab} and Masaru Ogura^{*ab}

Dependence of NH₃-SCR reaction rate on O₂ partial pressure was investigated at 473 K over Cu ion-exchanged MOR, MFI, CHA and *BEA zeolites with varying "Cu density in micropores". Among the zeolites, Cu-*BEA zeolite demonstrated promising potential as an effective catalyst for NH₃-SCR over a wide range of O₂ partial pressure.

Selective catalytic reduction of NO_x using NH₃ as a reducing agent (NH₃-SCR) is one of the most effective ways to remove NO_x from exhausts with O₂-rich compositions. A lot of catalysts for the reaction have been developed, such as V-based mixed oxides, Fe-zeolites, and Cu-zeolites.¹ Among the catalysts so far, Cu-zeolites exhibit a high reaction rate at a low NO₂ concentration (standard SCR) in a low temperature region (below 550 K).¹ Therefore, the current central trend of the study on the catalysts for NH₃-SCR is based on Cu-zeolites. Since the development of Cu/SSZ-13 zeolite catalyst with CHA topology, which exhibits a high reaction rate in wide temperature region, high selectivity of N₂, and a high durability under hydrothermal conditions,² a wide variety of zeolites were tested toward the application of NH₃-SCR.³

In the catalytic activity tests of NH₃-SCR, it is often the case that the O₂ concentration in the reaction feed is fixed at a certain value,^{3,4} and the effect of O₂ partial pressure (P_{O_2}) on the reaction rate has attracted little attention. The current application of NH₃-SCR is mainly the removal of NO_x emitted from diesel engine. The emission contains an excess amount of O₂ (typically 2–17%).⁵ A portion of the O₂ contained in the exhaust is steadily consumed over other catalysts for exhaust purification processes (*e.g.*, diesel oxidation catalyst; DOC and diesel particulate filter; DPF).⁶ The DOC catalyst plays a role in oxidative removal of unburned hydrocarbon (HC) and carbon monoxide (CO) using O₂. Particulate matter (PM) is trapped on the DPF and eliminated by catalytic combustion using O₂ and NO_x. In the exhaust purification system of diesel engine, such DOC and DPF units are generally mounted at the upstream of the SCR catalyst. The state-of-the-art SCR system of diesel

engines tends to be integrated to DPF to make the whole system compact.⁷ Moreover, the application of exhaust gas recirculation (EGR) system, which introduces a part of exhaust into engine cylinder to make the temperature of combustion decrease, resulting in the decrease of thermal NO_x, is in progress for the combustion process.⁸ These purification technologies will make the temperature of exhaust and the concentration of O₂ lower than they are.

On the other hand, a recent fundamental research⁹ has shown that the reaction rate for NH₃-SCR over Cu-SSZ-13 zeolite catalyst is greatly influenced by the P_{O_2} in a low P_{O_2} region with practical conditions ($P_{O_2} < 18$ kPa)⁵ at 473 K, where the overall rate of this reaction is largely affected by the oxidation of Cu ion on zeolites by O₂.¹⁰ It is shown in the literature⁹ that the SCR rate increases with increasing Cu volumetric density. However, the significant rate drop at the P_{O_2} below 15 kPa is a common behaviour of Cu-SSZ-13 zeolite regardless of its composition. Considering the recent trends on the composition of emission from practical diesel engines and the behaviour of Cu-SSZ-13 zeolite catalyst described above, it will be desired to widen the active window for exhaust composition at low reaction temperatures (~473 K) to pass future regulations.¹¹

Herein, a comparative study is conducted regarding NH₃-SCR reaction rate dependence on the P_{O_2} at 473 K over Cu ion-exchanged MOR, MFI, CHA and *BEA zeolites from the viewpoint of "Cu density in micropores"¹² to understand the effect of zeolite topology on the dependence.

Details on the preparation of the catalysts and the measurement of the reaction rates have been written in our previous reports.^{12,13} The reaction rate was calculated by determining the amount of NO converted to N₂ per second, which was divided by the amount of Cu in the catalyst. The O₂ concentration was kept at 5% during the pretreatment at 873 K, followed by cooling the temperature to 473 K. The cooling to 473 K was conducted under the feed of NH₃-SCR reactants and at least 45 min since the temperature was set to 473 K was ensured

^aInstitute of Industrial Science, The University of Tokyo, Komaba, Meguro, Tokyo 153-8505, Japan. E-mail: oguram@iis.u-tokyo.ac.jp

^bElements Strategy Initiative for Catalysts and Batteries, Kyoto University, Katsura, Kyoto 615-8520, Japan

† Electronic supplementary information (ESI) available. See DOI: 10.1039/d1ra00943e



to reach stable temperature and steady-state NO conversion. Then, the O₂ concentration was altered from 1 to 15%, and more than 10 min was needed to reach initial steady-state NO conversion at each targeted O₂ concentration. Formed NO₂ was transformed to NO by a NO₂ converter catalyst unit attached to a chemical luminescence NO_x analyser (HORIBA VA-3000); therefore, the NO conversion detected by the analyser was regarded as the NO_x conversion and the effect of background NO₂ was eliminated.

First of all, the catalytic activity of a reference Cu-SSZ-13 catalyst¹⁴ with a similar composition to the state-of-the-art commercial catalyst for NH₃-SCR was measured. It is reported that the catalyst has the composition of Si/Al and Cu/Al ratios ~9.5 and 0.3, respectively, corresponding 3.1 wt% Cu,¹⁵ whose Cu content is higher than that of any catalyst used in the report⁹ on dependence of NH₃-SCR rates on O₂ pressure.

Fig. 1a shows the rate dependence on P_{O₂} for NH₃-SCR per Cu ((mole NO to N₂) per (mole Cu) per s) by a kinetic measurement at 473 K over the reference Cu-SSZ-13 catalyst. Similar to “Langmuirian dependence” shown in the previous report by Jones *et al.*,⁹ a monotonic increase of SCR rate along with P_{O₂} was observed. Note that the dependence obtained in this work could be expressed by the Langmuir–Freundlich equation better than the Langmuir equation (Fig. S1†). The reaction order with respect to O₂ for NH₃-SCR per Cu was determined according to the following power law model equation.^{4a}

$$(\text{NH}_3\text{-SCR rate per Cu}) = A_0 \times \exp(-E_{\text{app}}/RT) \times (P_{\text{O}_2})^\alpha$$

The α in this equation expresses the reaction order for O₂. Fig. 1a was re-plotted to log–log axes (Fig. 1b) to know the slope corresponding to α . As shown in Fig. 1b, the log–log plot did not follow a linear relationship. It is observed that the slope of the plot decreased with increase in P_{O₂} in the reaction flow. This result shows that the reaction order for O₂ decreases with increase in P_{O₂}.

This phenomenon can be explained by the suggested redox mechanism between Cu⁺ and Cu²⁺ in the micropore of zeolites. The reduction of Cu²⁺ to Cu⁺ is thought to proceed by NH₃ + NO co-reductants,¹⁶ and the oxidation of Cu⁺ to Cu²⁺ is thought to proceed by O₂ oxidant.¹⁷ It has been observed by several *operando* analyses that both Cu⁺ and Cu²⁺ exist under a steady-state NH₃-SCR condition,¹⁸ although the ratio between two oxidation states depends both on the composition of Cu-zeolites and the

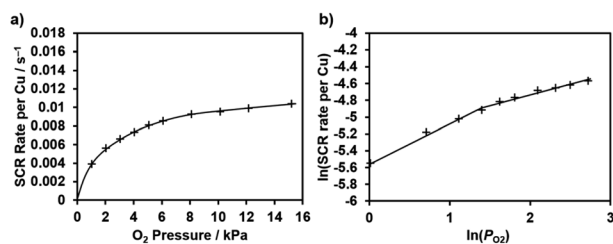


Fig. 1 (a) The dependence of NH₃-SCR rate per Cu at 473 K on O₂ pressure and (b) the log–log plot for the calculation of apparent O₂ order over the reference Cu-SSZ-13 zeolite.

Table 1 The reaction order for O₂ at 473 K over several P_{O₂} region

O ₂ partial pressure region/kPa	Reaction order for O ₂
1–4	0.46
5–15	0.14

reaction conditions. From these results, it has been suggested that the reaction rate is not solely limited by the rate for the Cu²⁺ reduction step (reduction half-cycle) nor Cu⁺ oxidation step (oxidation half-cycle).¹⁰ In other words, the reduction and oxidation half-cycles are kinetically relevant under the conditions below 523 K and at 5–20 kPa O₂ pressure over Cu-SSZ-13 zeolite.¹⁰

From the description above, the phenomenon observed in Fig. 1b can be understood as follows; the reaction is strongly influenced by the oxidation half-cycle under a low P_{O₂} reaction condition because the supply of oxidant is relatively insufficiency, and the oxidation half-cycle rate is improved with increasing the P_{O₂}. The reaction order for O₂ could be calculated in the low P_{O₂} region (≤ 4 kPa) and high P_{O₂} region ($5 \leq P_{\text{O}_2} \leq 15$ kPa). The results are shown in Table 1. The reaction order for O₂ decreased with increasing P_{O₂}, but did not reach to zero-order in the P_{O₂} region in this work. It is indicated from the results that the effect of oxidation half-cycle on the whole reaction rate remains in all the P_{O₂} region in this work, and the effect becomes stronger in a lower P_{O₂} region below 5 kPa than in the higher P_{O₂} region over this Cu-SSZ-13 catalyst. The apparent activation energy (E_{app}) for the reaction around 473 K calculated from the Arrhenius plots (Fig. S2†) was not changed obviously (Table 2) in the P_{O₂} region between 1 and 15 kPa. The value of the E_{app} was typical for the NH₃-SCR over Cu-zeolite catalysts.⁴ Therefore, it is confirmed that alteration of the reaction condition does not change the apparent E_{app} for kinetically relevant step(s).

The same measurements were conducted over the Cu-zeolite catalysts with MOR, MFI, *BEA, and CHA topologies that have similar cation density in micropores of zeolites and several Cu density in micropores.^{11,12} Cu-Zeolites with different topologies and cation density in micropores were applied in this study to minimize the contributions from factors other than the topology that can affect the NH₃-SCR rate.¹² Fig. 2 show the dependence of NH₃-SCR rate per Cu at 473 K on P_{O₂} over each topology. Cu density in micropores increases with light-to-dark shading (Table S1†). As shown in Fig. 2, monotonic increase of

Table 2 The apparent activation energy around 473 K in several O₂ pressure reaction over the reference Cu-SSZ-13 catalyst

O ₂ partial pressure/kPa	$E_{\text{app}}/\text{kJ mol}^{-1}$
1	49
5	44
15	44



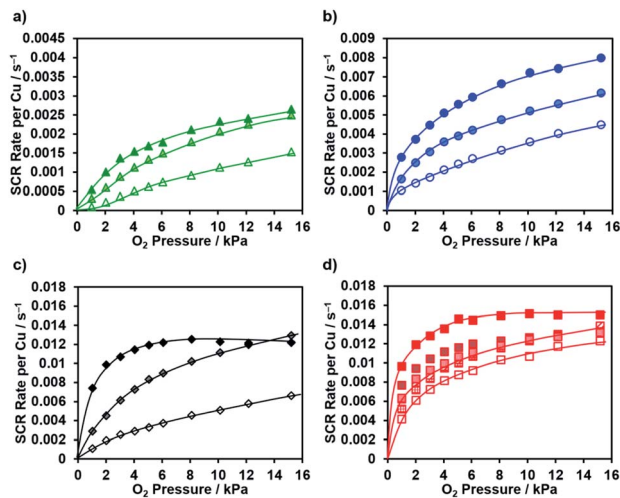


Fig. 2 The dependence of NH₃-SCR rate per Cu at 473 K on O₂ pressure over (a) MOR, (b) MFI, (c) CHA, and (d) *BEA zeolite catalyst with several Cu density in micropores. Cu density in micropores increases with light-to-dark shading.

SCR rate along with P_{O_2} increase similar to shown in Fig. 1a was observed over all Cu-zeolites. However, the changes of SCR rate along with both P_{O_2} and Cu density strongly affected by zeolite topologies and Cu density in micropores.

Cu-MOR zeolite applied in this study exhibited the lowest NH₃-SCR rate per Cu over all P_{O_2} region (Fig. 2a). Note that the scale of Y axis in Fig. 2a is as large as a quarter of Fig. 1a. A little increase was observed in both magnitudes and slopes of NH₃-SCR rate per Cu along with increasing Cu density in micropores. However, the rate was far smaller than that of the reference Cu-SSZ-13 zeolite catalyst, even with the higher Cu density.

Cu-MFI zeolite used in this study exhibited a higher NH₃-SCR rate per Cu over all P_{O_2} region than Cu-MOR zeolite (Fig. 2b). The scale of Y axis in Fig. 2b is as large as a half of that in Fig. 1a. In the case of the MFI zeolite, the increase was also observed in both magnitudes and slopes of NH₃-SCR rate per Cu with increasing Cu density in micropores. Both the reaction rate and its increase over Cu-MFI zeolite were larger than over Cu-MOR zeolite. However, the reaction rate over Cu-MFI zeolite was smaller than over the reference Cu-SSZ-13 zeolite catalyst regardless of Cu density in micropores. Even the Cu-MFI zeolite with Cu density in micropores at $7.4 (1000 \text{ \AA}^3)^{-1}$ (approximately 3 times as large as the reference Cu-SSZ-13 zeolite) did not represent an exception.

In the case of Cu-CHA zeolite, the increase behaviour in NH₃-SCR rate per Cu along with P_{O_2} was largely affected by the Cu density in micropores (Fig. 2c). The catalyst with a low Cu density in micropores showed relatively steady increase in NH₃-SCR rate per Cu along with P_{O_2} . On the other hand, the catalyst showed the rapid increase in NH₃-SCR rate per Cu in low P_{O_2} region, and the rate became constant in the higher P_{O_2} region (>6 kPa). Note that the slight decrease in NH₃-SCR rate per Cu of the Cu-CHA zeolite with the largest Cu density in micropores over 8 kPa P_{O_2} region is mainly caused by the increase in the formation of N₂O. Interestingly, the zeolites with Cu density in

micropores at 1.6 and $3.4 (1000 \text{ \AA}^3)^{-1}$ exhibited almost the same NH₃-SCR rate per Cu when P_{O_2} was at 15 kPa. This result suggests that they would reach the zero-order dependence on P_{O_2} , which means that the oxidation half-cycle does not determine the overall rate in the P_{O_2} region regardless of Cu density in micropores.

Among the Cu-zeolite catalysts, Cu-*BEA zeolite employed in this study exhibited high NH₃-SCR rate per Cu with relatively low dependence of on P_{O_2} (Fig. 2d). Moreover, the effect of Cu density in micropores of the catalyst was small on the behaviour of the rate along with P_{O_2} . Surprisingly, even the Cu-*BEA zeolite catalyst with Cu density in micropores at $0.76 (1000 \text{ \AA}^3)^{-1}$ (The sample shown as hollow red square symbol in Fig. 2d and described as B12 in Table S1†) exhibited a higher NH₃-SCR rate per Cu than the reference Cu-SSZ-13 catalyst with Cu density in micropores at $2.7 (1000 \text{ \AA}^3)^{-1}$ (Fig. S3a†). This difference was more obvious in lower temperature region (Fig. S3b†). In other words, the Cu-*BEA zeolite catalyst exhibited a high NH₃-SCR rate per Cu with low dependence on both Cu density in micropores and P_{O_2} in the temperature region below 473 K.

In the case of the zeolites other than Cu-CHA, the obvious deviation from a linear relationship following a Langmuir equation was observed in the dependence of SCR rate on P_{O_2} (Fig. S4†). To analyze the relationship, the Langmuir-Freundlich equation, which introduced the order on P_{O_2} as a correction factor to the Langmuir equation, was needed. From these results, it is suggested that the dependence of SCR rate on P_{O_2} over Cu-zeolites generally follows the Langmuir-Freundlich equation.

The reaction order for O₂ was calculated in a similar manner as the reference Cu-SSZ-13 catalyst in a low P_{O_2} region (≤ 5 kPa). The results were displayed as a function of Cu density in micropores (Fig. 3a). As shown in Fig. 3a, the reaction order for O₂ decreased with increase in the Cu density in micropores for all the zeolites investigated in this study. This result was consistent with the previous report on Cu-SSZ-13 zeolites with several Cu densities¹⁸ and can be understood by the increase in the rate for the oxidation half-cycle with increasing Cu density in micropores. When the reaction order for O₂ was compared among the Cu-zeolites with a similar Cu density in micropores, the tendency was observed that Cu-zeolite with a high reaction

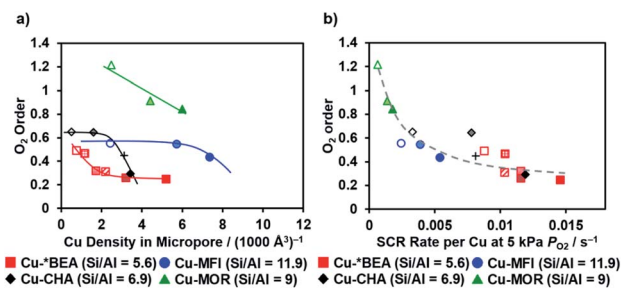


Fig. 3 The relationship between reaction order for O₂ in the O₂ pressure region (≤ 5 kPa) and the (a) Cu density in micropores or (b) SCR rate per Cu at 5 kPa O₂ over the MOR (\blacktriangle), MFI (\bullet), *BEA (\blacksquare), and CHA (\blacklozenge) zeolites. The cross symbol (+) shows the reference Cu-SSZ-13 zeolite.



rate showed a low reaction order for O₂ (Fig. 3b). This result means that the effect of P_{O₂} on the reaction rate is small over a catalyst with a high reaction rate such as Cu-CHA with high Cu density in micropores or Cu-*BEA.

Both the Cu density in micropores and P_{O₂} could play a role in the oxidation half-cycle in recently suggested mechanism of NH₃-SCR.¹⁷ Moreover, we have reported that the dependence of SCR rate against Cu density in micropores are related to the oxidation half-cycle in a previous report,¹² which investigated SCR rate at O₂ partial pressure of 5 kPa over the same catalysts tested in this study in detail. Thus, it can be assumed that the high NH₃-SCR rate of Cu-*BEA catalyst shown in this report is derived from the oxidation property for Cu⁺ ion by O₂ even insensitive to the P_{O₂}. However, detailed analysis using *operando* spectroscopic techniques will be necessary to elucidate the origin. It will be reported and discussed in the closest future.

Dependence of NH₃-SCR rate on P_{O₂} was investigated at 473 K over Cu ion-exchanged MOR, MFI, CHA and *BEA zeolites with several "Cu density in micropores". The reaction rate with respect to P_{O₂} was largely affected by the zeolite topology. Among the zeolites investigated here, Cu-*BEA zeolite catalyst exhibited a higher reaction rate regardless of the Cu density in micropores (or Cu loading) than a Cu-SSZ-13 reference catalyst in the whole range of Cu content tested in this study. The Cu-*BEA zeolite has a promising potential as the effective catalyst for NH₃-SCR in a wide range of P_{O₂}.

Conflicts of interest

There are no conflicts to declare.

Acknowledgements

This work was supported by "Elements Strategy Initiative for Catalysts & Batteries (ESICB)" of MEXT; Ministry of Education, Culture, Sports, Science and Technology, Japan, Grant Number JPMXP0112101003.

Notes and references

- 1 C. Görsmann, *Johnson Matthey Technol. Rev.*, 2015, **59**, 139.
- 2 J. H. Kwak, R. G. Tonkyn, D. H. Kim, J. Szanyi and C. H. F. Peden, *J. Catal.*, 2010, **275**, 187.
- 3 (a) M. Moliner, C. Franch, E. Palomares, M. Grillb and A. Corma, *Chem. Commun.*, 2012, **48**, 8264; (b) D. Jo, T. Ryu, G. T. Park, P. S. Kim, C. H. Kim, I.-S. Nam and S. B. Hong, *ACS Catal.*, 2016, **6**, 2443; (c) S. V. Priya, T. Ohnishi, Y. Shimada, Y. Kubota, T. Masuda, Y. Nakasaka, M. Matsukata, K. Itabashi, T. Okubo, T. Sano, N. Tsunoji, T. Yokoi and M. Ogura, *Bull. Chem. Soc. Jpn.*, 2018, **91**, 355; (d) J. Zhu, Z. Liu, L. Xu, T. Ohnishi, Y. Yanaba, M. Ogura, T. Wakihara and T. Okubo, *J. Catal.*, 2020, **391**, 346.
- 4 (a) F. Gao, E. D. Walter, E. M. Karp, J. Luo, R. G. Tonkyn, J. H. Kwak, J. Szanyi and C. H. F. Peden, *J. Catal.*, 2013, **300**, 20; (b) S. A. Bates, A. A. Verma, C. Paolucci, A. A. Parekh, T. Anggara, A. Yezerets, W. F. Schneider, J. T. Miller, W. N. Delgass and F. H. Ribeiro, *J. Catal.*, 2014, **312**, 87.
- 5 İ. A. Reşitoğ, K. Altinişik and A. Keskin, *Clean Technol. Environ. Policy*, 2015, **17**, 15.
- 6 B. K. Yun and M. Y. Kim, *Appl. Therm. Eng.*, 2013, **50**, 152.
- 7 G. Cavataio, J. R. Warner, J. W. Girard, J. Ura, D. Dobson and C. K. Lambert, *SAE Int. J. Fuels Lubr.*, 2009, **2**, 342.
- 8 M. Zheng, G. T. Reader and J. G. Hawley, *Energy Convers. Manage.*, 2004, **45**, 883.
- 9 C. B. Jones, I. Khurana, S. H. Krishna, A. J. Shih, W. N. Delgass, J. T. Miller, F. H. Ribeiro, W. F. Schneider and R. Gounder, *J. Catal.*, 2020, **389**, 140.
- 10 C. Paolucci, J. R. Di Iorio, W. F. Schneider and R. Gounder, *Acc. Chem. Res.*, 2020, **53**, 1881.
- 11 C. H. F. Peden, *J. Catal.*, 2019, **373**, 384.
- 12 Y. Ohata, H. Kubota, T. Toyao, K. Shimizu, T. Ohnishi, T. Moteki and M. Ogura, *Catal. Sci. Technol.*, 2021, DOI: 10.1039/D0CY01838D.
- 13 Y. Ohata, T. Nishitoba, T. Yokoi, T. Moteki and M. Ogura, *Bull. Chem. Soc. Jpn.*, 2019, **92**, 1935.
- 14 Detail on the preparation of the reference Cu-SSZ-13 is shown in the ESI for ref. 12. This sample is denoted as C905 in ref. 12.
- 15 J. Luo, F. Gao, K. Kamasamudram, N. Currier, C. H. F. Peden and A. Yezerets, *J. Catal.*, 2017, **348**, 291.
- 16 C. Paolucci, A. A. Parekh, I. Khurana, J. R. Di Iorio, H. Li, J. D. Albarracin Caballero, A. J. Shih, T. Anggara, W. N. Delgass, J. T. Miller, F. H. Ribeiro, R. Gounder and W. F. Schneider, *J. Am. Chem. Soc.*, 2016, **138**, 6028.
- 17 C. Paolucci, I. Khurana, A. A. Parekh, S. Li, A. J. Shih, H. Li, J. R. Di Iorio, J. D. Albarracin-Caballero, A. Yezerets, J. T. Miller, W. N. Delgass, F. H. Ribeiro, W. F. Schneider and R. Gounder, *Science*, 2017, **357**, 898.
- 18 C. Liu, H. Kubota, T. Amada, K. Kon, T. Toyao, Z. Maeno, K. Ueda, J. Ohyama, A. Satsuma, T. Tanigawa, N. Tsunoji, T. Sano and K. Shimizu, *ChemCatChem*, 2020, **12**, 3050.

